Studies of intramolecular electron and energy transfer using the *fac*-(diimine)$Re^{I}(CO)_3$ chromophore

Kirk S. Schanze, D. Brent MacQueen, Thomas A. Perkins and Leonardo A. Cabana
Department of Chemistry, University of Florida, Gainesville, FL 32611 (USA)

(Received 29 January 1992)

CONTENTS

A. Introduction . . . 64
B. (b)$Re^{I}(CO)_3$L complexes. Synthesis and photophysical properties . . . 64
(i) Synthesis . . . 64
(ii) Photophysics and excited-state redox properties . . . 65
C. Photoinduced intramolecular electron transfer in Re(I) C-Q complexes . . . 69
(i) Kinetic and thermodynamic considerations . . . 69
(ii) Dependence of k_{ET} on ΔG_{ET} in (b)$Re(CO)_3$PyDMAB complexes . . . 71
(iii) Back electron transfer in (b)$Re(CO)_3$PyPTZ complexes . . . 74
(iv) Long-range photoinduced electron transfer across peptide spacers . . . 75
(v) Donor-to-metal electron transfer across a rigid organic spacer . . . 78
(vi) Comparisons of forward electron transfer rate data . . . 79
(vii) Comparisons of back electron transfer rate data . . . 82
D. Intramolecular energy transfer in Re(I) complexes . . . 83
E. Concluding remarks . . . 85
Acknowledgements . . . 86
References . . . 86

ABBREVIATIONS FOR DIIMINE LIGANDS

tmb	4,4′,5,5′-tetramethyl-2,2′-bipyridine
dmb	4,4′-dimethyl-2,2′-bipyridine
bpy	2,2′-bipyridine
4-dab	4,4′-bis(*N*,*N*-diethylcarbamido)-2,2′-bipyridine
5-dab	5,5′-bis(*N*,*N*-diethylcarbamido)-2,2′-bipyridine
deb	4,4′-bis(carboethoxy)-2,2′-bipyridine
bpz	2,2′-bipyrazine

Correspondence to: K.S. Schanze, Department of Chemistry, University of Florida, Gainesville, FL 32611, USA.

0010-8545/93/$24.00

A. INTRODUCTION

Chromophore-quencher (C-Q) molecules contain a light-absorbing moiety covalently linked to a molecular unit which quenches the electronically excited state of the chromophore, usually by intramolecular electron or energy tansfer (e.t. or E_nT, respectively). C-Q molecules have played a prominent role in elucidating the dependence of the rate for e.t. or E_nT on factors such as donor–acceptor separation distance, thermodynamic driving force, medium, and the molecular structure of the spacer which connects the donor and acceptor [1–19]. Most studies have focused on C-Q systems which utilize organic chromophores such as porphyrins and aromatic hydrocarbons [1–19]; however, recently there has been an increasing number of studies concerning intramolecular e.t. and E_nT in C-Q molecules which utilize a transition metal chromophore [20–50]. Most of these transition metal-based C-Q systems utilize either $Ru^{II}(b)_3$ or *fac*-$(b)Re^{I}(CO)_3$ chromophores (where b is a bidentate diimine ligand such as 2,2′-bipyridine). Both of these chromophores are useful because they have luminescent excited states which are based on $d\pi(M) \rightarrow \pi^*$ (diimine) metal-to-ligand charge transfer (MLCT). However, the Re(I) system is particularly well suited for studies of e.t. and E_nT in C-Q molecules because of a unique combination of features that include a convenient and versatile synthetic chemistry, thermal and photochemical stability, luminescent MLCT excited state, and tunable excited state energy and redox potentials.

The objective of the present review is to summarize the results of recent studies of C-Q systems in which the *fac*-$(b)Re^{I}(CO)_3$ unit has been utilized as the photoactive unit. Several issues are covered, including (1) the chemical and photophysical properties of the *fac*-$(b)Re^{I}(CO)_3$ chromophore which are relevant to the synthesis of C-Q molecules and the study of intramolecular e.t. or E_nT. (2) studies concerning the distance and driving-force dependence of e.t. in Re(I)-based C-Q complexes, and (3) studies of the driving force dependence of intramolecular triplet E_nT. While most of the work which is described has been carried out by the author's research group, related work carried out in other laboratories will also be discussed.

B. $(b)Re^{I}(CO)_3L$ COMPLEXES. SYNTHESIS AND PHOTOPHYSICAL PROPERTIES

(i) Synthesis

The starting material for $(b)Re^{I}(CO)_3L$ complexes (where L is a monodentate σ-donor, π-acceptor ligand such as a substituted pyridine) is *fac*-$(b)Re^{I}(CO)_3Cl$, which can be readily prepared from $ClRe(CO)_5$ and a variety of diimine ligands in high yield [46]. Several methods have been utilized to prepare the target $(b)Re^{I}(CO)_3L$ complexes from the $(b)Re^{I}(CO)_3Cl$ precursor. One involves preparation and isolation of the complex $(b)Re^{I}(CO)_3(CF_3SO_3)$ [51], which is then reacted with approximately one equivalent of the ligand, L, in refluxing EtOH or THF [49]. A

problem with this approach is that the immediate product of the reaction is a trifluoromethane sulfonate salt $[(b)Re^{I}(CO)_3L^{-}][CF_3SO_3^{-}]$. These salts typically have RF = 0 on alumina or silica gel, which precludes the use of thin-layer chromatography (TLC) to follow the reaction. The method of choice in our laboratory is to convert the chloro complex directly to the L-substituted complex by reaction with a slight excess of the monodentate ligand in the presence of excess $AgPF_6$ [46]:

$$(b)Re^{I}(CO)_3Cl + 1.2eq.L \xrightarrow[DMF,\ 70\ C]{3eq\,AgPF_6} [(b)Re^{I}(CO)_3L^{+}][PF_6^{-}] + AgCl \quad (1)$$

This reaction is conveniently followed by using either alumina (20% CH_3CN/CH_2Cl_2 eluant) or silica gel (5% $MeOH/CH_2Cl_2$ eluant) TLC to monitor the disappearance of the starting material and product formation; yields of the purified $[(b)Re^{I}(CO)_3L^{+}][PF_6^{-}]$ complexes typically range from 20 to 50%.

(ii) Photophysics and excited-state redox properties

Wrighton et al. discovered the unique photophysical properties of the $(b)Re^{I}(CO)_3$ chromophore [52–54]. In a study of a series of substituted 1,10-phenanthroline complexes, they observed moderately long-lived luminescence in fluid solution at 25°C which was assigned to a $d\pi$ (Re)$\rightarrow\pi^*$ (phenanthroline) MLCT excited state [52]. The MLCT assignment was supported by the fact that the emission energy decreased as the electron acceptor capacity of the phenanthroline was increased.

More recently, we have examined the photophysical and electrochemical properties of the series of complexes $(b)Re(CO)_3PyB$ [46] (see Fig. 1 for structures). These complexes contain a series of substituted diimine ligands which were specifically selected because of their widely varying electron acceptor capacity (LUMO energy). Interestingly, the photophysical and redox properties of the $(b)Re^{I}(CO)_3$ chromophore vary strongly, but systematically, as the diimine ligand is varied. Table 1 contains a summary of emission maxima (E_{em}), emission lifetimes (τ_{em}), and ground and excited-state redox potentials for this series. Each complex displays a moderately intense, broad emission band in fluid solution at 25°C which is assigned to the $d\pi(Re)\rightarrow\pi^*$ (diimine) MLCT excited state. The MLCT assigment is supported by correlation of $E_{0,0}$ with the ground state reduction potentials (Fig. 2), which correspond to reduction of the coordinated diimine ligands. Figure 2 also highlights the relatively large change in $E_{0,0}$ which accompanies variation of the diimine ligand.

Another feature concerning the photophysical data for this series is that τ_{em} decreases as E_{em} decreases (Fig. 2). In order to gain more insight concerning the effect of E_{em} on the lifetime of the MLCT excited state in Re(I) complexes, Meyer and co-workers examined the effect of E_{em} on the radiative and non-radiative components of the excited state decay rate (k_r and k_{nr}, respectively) for the series of complexes, $(b)Re^{I}(CO)_3Cl$ [55]. The results of their study are summarized in Fig. 3,

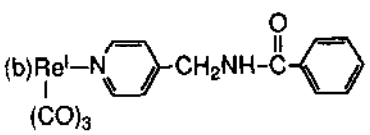

(b)Re(CO)$_3$PyB

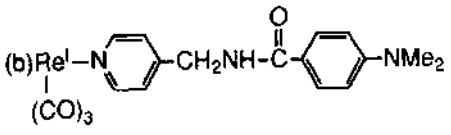

(b)Re(CO)$_3$PyDMAB

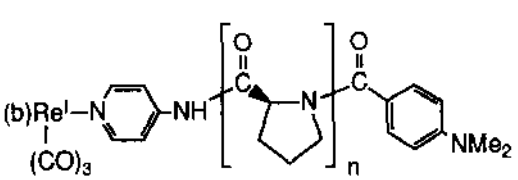

(bpy)Re(CO)$_3$(Pro)$_n$DMAB

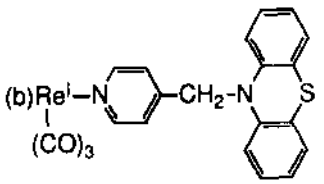

(b)Re(CO)$_3$PyPTZ

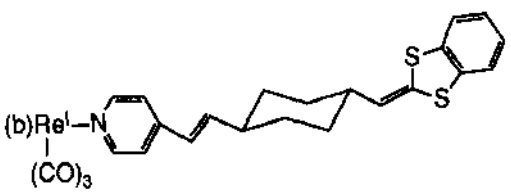

(b)Re(CO)$_3$CH-DTF

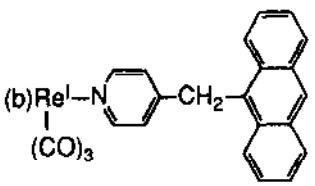

(b)Re(CO)$_3$PyAn

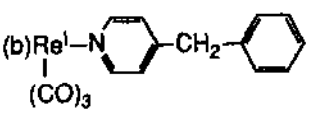

(b)Re(CO)$_3$PyPh

Fig. 1. Structures and abbreviations for Re(I) complexes discussed in text. The ligand b is a bidentate diimine ligand such as 2,2-bipyridine (see text for ligand abbreviations). The stereochemistry at Re(I) is *facial*.

where $\ln(k_{nr})$ and $\ln(k_r)$ are plotted as functions of E_{em}. Note that $\ln(k_{nr})$ decreases linearly as E_{em} increases, while $\ln(k_r)$ remains relatively constant. The linear dependence of $\ln(k_{nr})$ on E_{em} is explained by the theory of highly exothermic, non-radiative decay processes, and the effect has been termed the "Energy Gap Law" [56]. By analogy with the (b)Re^{I}(CO)$_3$Cl system, we believe that the concomitant decrease in τ_{em} and E_{em} which is observed for the (b)Re(CO)$_3$PyB series (Fig. 2) arises because of the effect of E_{em} on k_{nr}.

By using the photophysical and redox data compiled for the (b)Re(CO)$_3$PyB

TABLE 1

Photophysical and redox data for (b)Re(CO)$_3$PyB complexes[a,b]

Ligand	$E_{em}(E_{0,0})$/cm^{-1}[c]	τ_{em}/ns	$E_{1/2}(Re^{+/0})$/V	$E_{1/2}(Re^{+/2+})$/V	$E_{1/2}(*Re^{+/0})$/V[d]	$E_{1/2}(*Re^{+/2+})$/V[e]
tmb	18400 (20700)	1450	−1.387	+1.701	+1.18	−0.87
dmb	17400 (19700	269	−1.245	+1.760	+1.20	−0.68
bpy	16900 (19200)	211	−1.164	+1.806	+1.22	−0.58
4-dab	16100 (18500)	107	−1.001	+1.858	+1.30	−0.44
deb	15300 (17300)	75	−0.667	+1.965[f]	+1.48	−0.18
bpz	14600 (16800)	27	−0.717	+1.982[f]	+1.36	−0.10

[a] All data for CH_3CN solutions.

[b] All redox potentials are relative to the saturated sodium calomel electrode (+0.236 V vs. NHE).

[c] E_{em} is the energy of the band maximum; $E_{0,0}$ is the 0-0 emission energy (corrected for photomultiplier response) which is estimated by using a Franck–Condon analysis to fit the emission band [46].

[d] Excited state reduction potentials calculated by: $E_{1/2}(*R^{+/0}) = E_{1/2}(Re^{+/0}) + E_{0,0}$.

[e] Excited state oxidation potentials calculated by: $E_{1/2}(*Re^{+/2+}) = E_{1/2}(Re^{+/2+}) - E_{0,0}$.

[f] Quasi-reversible wave.

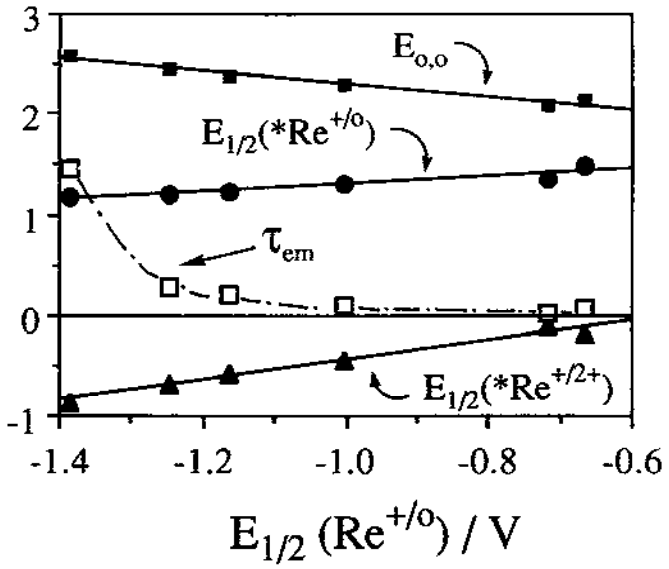

Fig. 2. Plot of $E_{0,0}$, $E_{1/2}(*Re^{+/0})$, $E_{1/2}(*Re^{+/2+})$, and τ_{em} as a function of the $E_{1/2}(Re^{+/0})$ for the (b)Re(CO)$_3$PyB series in CH_3CN solution. Units: $E_{1/2}(*Re^{+/0})$ and $E_{1/2}(*Re^{+/2+})$ in V vs. SSCE. $E_{0,0}$ in eV, and τ_{em} in μs. Note that the first reduction of the complexes, $E_{1/2}(Re^{+/0})$, corresponds to reduction of the diimine ligand.

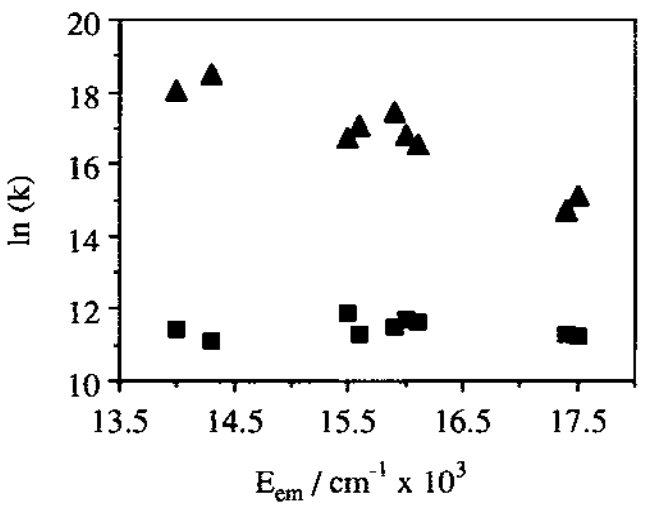

Fig. 3. Plots of ln k_{nr} (▲) and ln k_r (■) as functions of emission energy for a series of (diimine)Re(CO)$_3$Cl complexes (data from ref. 55).

complexes, excited-state redox potentials have been calculated (Table 1). Several points are of interest regarding these data. First, in general, the photoexcited (b)$Re^I(CO)_3$ chromophore is a comparatively strong oxidant; however, it is a relatively weak reductant. Second, the excited state redox potentials vary systematically as the

diimine ligand changes. This variation is also illustrated in Fig. 2, where the excited state potentials are plotted as a function of the ground-state reduction potential. An important point to note is that $E_{1/2}(*Re^{+/0})$ varies by approximately 300 mV across the series, while $E_{1/2}(*Re^{+/2+})$ varies over a 900 mV range.

A major thrust of our work on the (b)$Re^{I}(CO)_3$ chromophore has involved its use in C-Q molecules designed to allow the study of intramolecular e.t. and E_mT [43–49]. As a result, it is important to point out the way in which the nominal photophysical properties impact the study of C-Q complexes which incorporate the Re(I) center. The first point which must be considered is that the (b)$Re^{I}(CO)_3$ chromophore is a stronger oxidant than a reductant. Because of this feature, in studies of intramolecular e.t. in Re(I)-based C-Q compounds the quencher (Q) is typically an electron donor (D). This allows for moderately exothermic photoinduced e.t., even with only moderately strong donors (e.g. $E_{1/2}(D^{0/+})$ ranging from +0.5 to +1.2 V vs. SCE). Second, because $E_{1/2}(*Re^{+/0})$ can be varied by changing the diimine ligand, it is possible to study systematically the effect of the free energy change for e.t. (ΔG_{ET}) on the rate of intramolecular e.t. in Re(I)-based C-Q compounds. A third important feature of the Re(I) chromophore is that E_{em} can be systematically "tuned" over a relatively wide range by varying the diimine ligand (Fig. 2). This tunability provides an important tool for the study of driving force effects on the rate of excited state energy transfer (see Sect. D).

C. PHOTOINDUCED INTRAMOLECULAR ELECTRON TRANSFER IN Re(I) C-Q COMPLEXES

(i) Kinetic and thermodynamic considerations

As noted above, in studies of e.t. in Re(I)-based C-Q complexes, the covalently linked quencher is usually an electron donor [24–27,43–46]. Thus, a generic Re(I)-based C-Q complex can be abbreviated as (b)Re^{I}-D, where D represents an electron donor. Figure 4 shows an excited-state diagram which illustrates the kinetic and thermodynamic parameters that are important for such a system. Photoexcitation

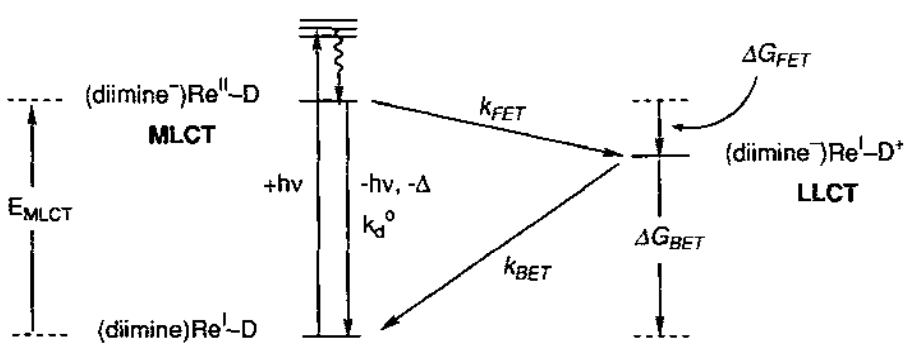

Fig. 4. General excited-state diagram for an electron donor-substituted Re(I) complex.

in the near-UV region rapidly produces the MLCT excited state, which can subsequently decay by either of two paths: (1) normal radiative and non-radiative decay, with rate k_d^0; (2) intramolecular forward e.t., with rate k_{FET} and thermodynamic driving force ΔG_{FET}. Importantly, the forward e.t. quenching step involves transfer of an electron from the donor to the electron-deficient metal center, which results in formation of a ligand-to-ligand charge transfer (LLCT) state. In the LLCT state, the odd-electron is localized on the diimine acceptor ligand and the positive (hole) is localized on the organic donor. Decay of the LLCT state occurs by back e.t., with rate k_{BET} and driving force ΔG_{BET}. Importantly, this process is not simply the reverse of the forward (quenching) e.t. step: in back e.t., the diimine radical anion is the electron donor and the donor radical cation is the electron acceptor. Because of this difference, Franck–Condon and electronic coupling terms are not expected to be the same for forward and back e.t.

The thermodynamics for forward and back e.t. in (b)Re-D complexes can be estimated from electrochemical and spectroscopic data by using the expressions

$$\Delta G_{FET} \approx E_{1/2}(D/D^{+\cdot}) - E_{1/2}(Re^{\cdot 0}) - E_{0,0} \tag{2}$$

$$\Delta G_{BET} \approx E_{1/2}(Re^{-/0}) - E_{1/2}(D/D^{+\cdot}) \tag{3}$$

where $E_{1/2}(Re^{-/0})$ is the first reduction potential of the (b)$Re^{I}(CO)_3$ chromophore, $E_{1/2}(D/D^{+\cdot})$ is the first oxidation potential of the donor, and $E_{0,0}$ is the 0–0 energy of the MLCT excited state, which can be estimated by using emission spectroscopy [3,57]. Note that a coulombic interaction term has been left out of these expressions. This is justified because, if the overall +1 charge of the (b)$Re^{I}(CO)_3L$ chromophore is taken into account, photoinduced intramolecular e.t. is a charge shift reaction.

The rate constant for forward e.t. in (b)$Re^{I}(CO)_3$-D complexes is determined by time-resolved emission measurements. In a (b)$Re^{I}(CO)_3$-D complex, the total decay rate of the excited state (k_d) is given by the sum of the "normal" decay rate of the MLCT state and the rate of forward e.t. (eqn. (4a)). Rearranging eqn. (4a) and substituting inverse lifetimes ($1/\tau$) in place of decay rate

$$k_d = k_{FET} + k_d^0 \tag{4a}$$

$$k_{FET} = \frac{1}{\tau_{em}} - \frac{1}{\tau_{em}^0} \tag{4b}$$

constants leads to eqn. (4b), in which τ_{em} is the emission lifetime of the (b)$Re^{I}(CO)_3$-D complex, and τ_{em}^0 is the emission lifetime of a suitable "model" complex, which is structurally identical to the (b)$Re^{I}(CO)_3$-D complex, but lacks the electron donor functional group. The assumption which is required for eqn. (4b) to be correct is that k_d^0 is identical for the (b)$Re^{I}(CO)_3$-D and the model complex. Lifetime studies of various model complexes indicate that this assumption is valid when the model complex is carefully selected [44,49].

The factors which ultimately limit the dynamic range of forward e.t. rates that

can be measured are (1) the temporal response of the emission lifetime apparatus, and (2) the "normal" MLCT decay rate (k_d^0). By using flashlamp-based time-correlated single photon counting (TCSPC), MLCT emission lifetimes can be routinely measured to approximately 200 ps; this places an upper limit of ca. 5×10^9 s^{-1} on k_{FET}, which can be measured in (b)Re^{I}(CO)$_3$-D complexes. Assuming that the typical experimental error in emission lifetime values obtained by TCSPC is $\pm 5\%$, the lower limit on k_{FET} which can be determined is approximately $0.05 \times k_d^0$. Due to the fact that k_d^0 varies widely depending upon the diimine ligand (see Table 1), the lower limit on k_{FET} depends upon the particular (b)Re^{I}(CO)$_3$-D complex that is being considered: however, the range is approximately 10^5–10^7 s^{-1}.

The rate for back e.t. in (b)Re^{I}(CO)$_3$-D complexes is determined by using laser flash photolysis (LFP) to monitor the decay rate of the LLCT state. For most of the (b)Re^{I}(CO)$_3$-D systems which have been studied to date, the donor radical cation (D$^{+\cdot}$) which is present in the LLCT state, (b$^{-\cdot}$)Re^{I}(CO)$_3$-D$^{+\cdot}$, gives rise to a moderately strong visible absorption that can be conveniently monitored in the LFP experiment [25,45,46]. The limits that constrain the dynamic range of k_{BET} values which can be determined are: (1) the LLCT state must be produced in sufficient quantum yield so that it can be easily observed by LFP; (2) k_{BET} must be slower than k_{FET} so that the concentration of the LLCT state is sufficient to allow its detection by LFP; (3) the temporal response of the LFP instrumentation. Luckily, for most (b)Re^{I}(CO)$_3$-D complexes studied to date, the first two factors do not play a role, and the only limitation is governed by the minimum time resolution of the LFP instrumentation.

(ii) Dependence of k_{ET} on ΔG_{ET} in (b)Re(CO)$_3$PyDMAB complexes

One of the most comprehensive studies of the effect of free energy on the rate of photoinduced intramolecular e.t. in transition metal-based C-Q systems was recently carried out using the series of complexes (b)Re(CO)$_3$PyDMAB [46]. In this series, the dependence of k_{FET} on ΔG_{FET} and k_{BET} on ΔG_{BET} was determined in several solvents. Forward e.t. rate constants were determined by measuring emission lifetimes for the (b)Re(CO)$_3$PyDMAB complexes and the corresponding (b)Re(CO)$_3$PyB complexes and using eqn. (4b) to calculate k_{BET}. Back e.t. rates were determined by using LFP to monitor directly the decay of the LLCT state which is formed by foward e.t. quenching of the MLCT excited state. The kinetic results are displayed in a series of graphs in Figs. 5 and 6.

Several key features emerged from this study. First, for this series of complexes, forward e.t. is weakly exothermic and back e.t. is strongly exothermic; as a result, forward e.t. falls in the Marcus "normal" free energy region and back e.t. falls in the Marcus "inverted" region [58–60]. The results illustrated in Figs. 5 and 6 indicate that the general trends in k_{FET} and k_{BET} are qualitatively consistent with the predic-

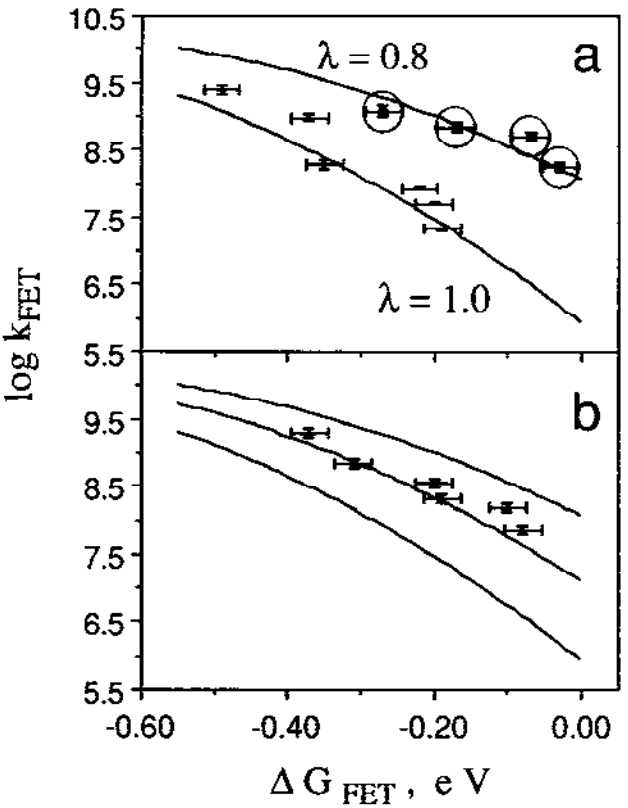

Fig. 5. Plots of log k_{FET} vs. ΔG_{FET} for the (b)Re(CO)$_3$PyDMAB complexes in three solvents. (a) Uncircled points in MeCN solution, circled points in CH_2Cl_2 solution. (b) Data in DMF solution. Solid lines calculated using eqn.(5) with parameters given in text.

tions of Marcus theory: k_{FET} increases as ΔG_{FET} becomes *more* exothermic, while k_{BET} increases as ΔG_{BET} becomes *less* exothermic.

Second, there is a comparatively strong solvent effect on k_{FET}; for comparable ΔG_{FET} values, k_{FET} increases as the solvent polarity decreases. Analysis of the forward e.t. rate data using the semi-classical Marcus expression (eqn. (5)) provides a very reasonable explanation for the solvent

$$k_{ET} = \nu_n \kappa_{el} \kappa_n \tag{5a}$$

$$\nu_n \kappa_{el} = \left\{\frac{2H_{AB}^2}{h}\right\}\left\{\frac{\pi^3}{\lambda k_B T}\right\}^{1/2} \tag{5b}$$

$$\kappa_n = \exp\left\{-\frac{(\Delta G_{ET} + \lambda)^2}{4\lambda k_B T}\right\}$$

dependence of k_{FET}. The semi-classical expression describes the relationship between k_{ET} and ΔG_{ET}, the reorganization energy (λ), and the "maximum rate" ($\nu_n \kappa_{el}$), which

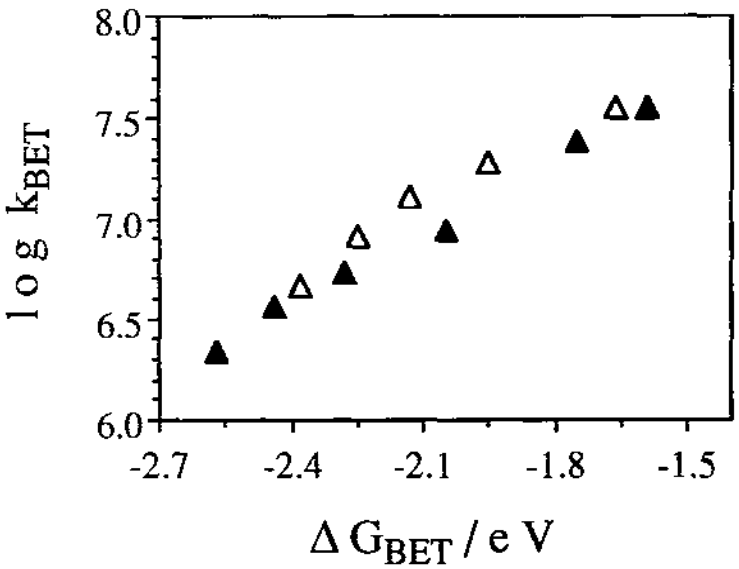

Fig. 6. Plot of log k_{BET} vs. ΔG_{BET} for (b)Re(CO)$_3$PyDMAB complexes in CH_2Cl_2 solution (▲) and MeCN (△) solution.

is the product of an effective nuclear vibration frequency and the electronic transmission coefficient [58,59]. Note that the maximum rate is proportional to the square of the donor–acceptor electronic coupling matrix element (H_{AB}). The solid lines drawn in Fig. 5 were calculated by using eqn. (5) with $\nu_n \kappa_{el} = 1.3 \times 10^{10}$ s^{-1} (H_{AB} = 7.5 cm^{-1}) and $\lambda = 0.8$ eV (CH_2Cl_2), 0.9 eV (DMF), and 1.0 eV (CH_3CN). This analysis suggests that the solvent dependence in k_{ET} is due mainly to the solvent dependence of λ.

It is of interest to compare the solvent dependence of λ that is implied by the fits of the experimental rate data to that predicted by using the Marcus–Hush two-sphere dielectric continuum model (eqn. (6)) to calculate the solvent dependence of the outer-sphere component of the reorganization energy, λ_0 [61,62]:

$$\lambda_0 = e^2 \left[\frac{1}{2r_D} + \frac{1}{2r_A} - \frac{1}{r_{DA}} \right] \left[\frac{1}{\varepsilon_{op}} - \frac{1}{\varepsilon_s} \right] \tag{6}$$

The dielectric continuum model expresses the relationship between λ_0, and the radii of the donor and acceptor (r_D and r_A, respectively), the donor–acceptor separation (r_{DA}), and static and optical dielectric constants of the solvent (ε_{op} and ε_s, respectively). Crystal structure coordinates for the (bpy)Re(CO)$_3$(pyridine) moiety and the SYBYL molecular modelling program were used to estimate r_D, r_A, and r_{DA} for the (b)Re(CO)$_3$DMAB complexes (3.2, 4.0, and 11.0 Å, respectively). Using these values, eqn. (6) predicts that λ_0 is 0.99 eV in CH_2Cl_2, 1.20 eV in DMF, and 1.37 eV in CH_3CN. These estimated values are clearly larger than those given by the fits of the

experimental data shown in Fig. 5, especially considering the fact that the calculated reorganization energies do not include the inner sphere component. Despite this lack of quantitative agreement, two facts are of interest with respect to the calculation using eqn. (6). Analysis of the solvent dependence of the intervalence charge transfer (ICT) absorption for mixed valence metal complexes has shown that λ_o values calculated by eqn. (6) are consistently 20–30% larger than the experimental values [63]. Thus, the results obtained by using photoinduced e.t. in the (b)$Re(CO)_3$DMAB series are consistent with the findings of the ICT experiments since, in both cases, the experimental values of λ are lower than predicted by eqn. (6). It is important to note, however, that the relative solvent dependence in λ that is predicted by eqn. (6) is in comparatively good agreement with that which is implied by the fits in Fig. 5.

The third important feature is that the (inverted) dependence of k_{BET} on ΔG_{BET} in the (b)$Re(CO)_3$PyDMAB complexes is substantially weaker than has been observed in studies of highly exothermic, inverted region e.t. reactions in organic-based donor–acceptor and C-Q compounds [8,41,64–66]. Importantly, a similar relatively weak dependence of k_{BET} on ΔG_{BET} was observed in a recent study carried out by Meyer and co-workers on the structurally similar family of donor-substituted complexes, (b)$Re(CO)_3$PyPTZ (vide infra) [26,27]. These facts imply that back e.t. in the donor-substituted Re(I) complexes is unusual compared with the organic-based systems. One possible explanation for the comparatively weak dependence of k_{BET} on ΔG_{BET} in the (b)$Re(CO)_3$PyDMAB series is that due to the structural complexity at the metal center, the number of high-frequency vibrational modes which are coupled to back e.t. is larger than in the organic systems. Specifically, it is possible that CO-based vibrations are coupled to back e.t., in addition to diimine- and donor-based C=C modes. In effect, the increase in the number of high-frequency acceptor modes may act to "flatten" the dependence of k_{BET} on ΔG_{BET} in the metal complex based C-Q systems. (Note that in a single high-frequency mode approximation, a larger number of high-frequency modes coupled to e.t. would be manifested as a larger inner sphere reorganization energy.)

An alternative explanation for the comparatively weak dependence of k_{BET} on ΔG_{BET} which is observed for the (b)$Re(CO)_3$PyDMAB complexes may be that e.t. is not the rate-determining step for decay of the charge-separated, LLCT state. It is possible that the LLCT state retains triplet spin character after it is formed by forward e.t. quenching of the triplet MLCT excited state [67]. In this case, intersystem crossing (ISC) must occur prior to back e.t., and the free energy dependence which is observed may arise from variation in the rate of ISC with the diimine ligand [46].

(iii) Back electron transfer in (b)$Re(CO)_3$PyPTZ complexes

In another recent study, Meyer and co-workers examined photoinduced intramolecular e.t. in the series of complexes (b)$Re(CO)_3$PyPTZ [24–27]. Since phenothiazine (PTZ) is a very good electron donor ($E_{1/2}(PTZ/PTZ^+) \approx +0.7$ V vs. SCE),

photoexcitation of the (b)$Re^{I}(CO)_3$ chromophore leads to the sequence of forward and back e.t. reactions shown in Fig. 4 (where D = PTZ). As in the (b)$Re(CO)_3$PyDMAB series, ΔG_{FET} and ΔG_{BET} were varied by changing the substituents on the diimine ligand. Because of the good donor properties of PTZ, ΔG_{FET} is moderately exothermic in this series ($\lesssim -0.5$ eV); as a result, k_{FET} was too large to be determined by using fluorescence lifetime techniques. However, k_{BET} was determined for ΔG_{BET} ranging from -1.4 to -2.15 eV by monitoring the decay of the LLCT state, $(b^{-\cdot})Re(CO)_3Py(PTZ^{+\cdot})$, by using ns laser flash photolysis. The rate of back e.t. in the (b)$Re(CO)_3$PyPTZ series displays an inverted dependence on ΔG_{BET}. Quite remarkably, the correlation between k_{BET} and ΔG_{BET} for this series is virtually superimposable on the correlation established for the (b)$Re(CO)_3$PyDMAB series; a comparison of the rate data for the two series is provided in Fig. 8 (see below).

(iv) Long-range photoinduced electron transfer across peptide spacers

In another recent study, the distance dependence of the rate of photoinduced e.t. from a dimethylaniline electron donor to the photoexcited (bpy)$Re^{I}(CO)_3$ chromophore was examined by varying the length of the peptide spacer in the three-member series which is comprised of (bpy)$Re(CO)_3$PyDMAB, (bpy)$Re(CO)_3(Pro)_1$DMAB, and (bpy)$Re(CO)_3(Pro)_2$DMAB [43,44,49]. The proline peptide spacers were selected for these studies for several reasons.

(1) Techniques for the synthesis of relatively short peptide oligomers are highly refined, allowing rapid preparation of peptide-based spacers of varying lengths [68,69].

(2) The pyrrolidine ring places significant conformational restrictions on oligomers which are comprised of proline. A variety of studies have demonstrated that, in protic solvents, proline oligomers exist predominantly in extended conformations and the dynamics of conformational change are slow [19,43,68,70].

(3) The use of peptide spacers in model systems for long-range e.t. allows insight to be gained concerning the role of the peptide in mediating through-bond electronic coupling between electron donors and acceptors in redox proteins. [70–74]

The free energy for forward e.t. (ΔG_{FET}) in the proline-bridged complexes is approximately -0.23 eV. The kinetics of forward e.t. as a function of peptide spacer length were determined from the MLCT emission lifetimes of the three donor-substituted complexes (bpy)$Re(CO)_3$PyDMAB, (bpy)$Re(CO)_3(Pro)_1$DMAB, and (bpy)$Re(CO)_3(Pro)_2$DMAB, and corresponding non-donor substituted model complexes by using eqn. (4b). Temperature-dependent emission lifetime studies were also carried out, allowing calculation of the activation enthalpy and entropy for forward e.t. ($\Delta H^{\ddagger}_{FET}$ and $\Delta S^{\ddagger}_{FET}$, respectively). The experimental rate data are summarized in Table 2. Note that k_{FET} displays a comparatively strong distance dependence, decreasing by approximately a factor of 20 with each added proline residue. Another

TABLE 2

Forward electron transfer rate data for proline-bridged complexes[a]

Complex	k_{FET}/s^{-1}	$\Delta H^{\neq}_{FET}$/kcal mol^{-1}	$\Delta S^{\neq}_{FET}$/eu
(bpy)Re(CO)$_3$PyDMAB	$9.8(0.3) \times 10^7$	3.3(0.3)	−10.7(1.5)
(bpy)Re(CO)$_3$(Pro)$_1$DMAB	$5.3(0.5) \times 10^6$	4.0(0.7)	−14(2)
(bpy)Re(CO)$_3$(Pro)$_2$DMAB	$3.7(2) \times 10^5$	4.1(1.8)	−19(4)

[a]All values represent averages; standard deviations are given in parentheses. All measurements carried out in MeOH solution. $\Delta G_{FET} \approx -0.23$ eV.

interesting feature is that, as the number of peptide spacers increases, $\Delta H^{\neq}_{FET}$ increases only slightly, while $\Delta S^{\neq}_{FET}$ becomes increasingly more negative.

The distance dependence of the rate of e.t. arises from attenuation of both the nuclear and electronic terms (κ_n and κ_{el}, eqn. (5)) with increasing separation distance. Superexchange theory is often used to model the decay of the electronic coupling with increasing donor–acceptor separation; this theory predicts that H_{AB}, and therefore κ_{el}, decreases exponentially with increasing donor–acceptor separation [75,76]:

$$\kappa_{el}(r) = \kappa^0_{el} \exp\{-\beta_{el}(r - r_0)\} \tag{7}$$

In eqn. (7), κ^0_{el} is the electronic transmission coefficient when the donor and acceptor are separated by the sum of their van der Waals radii, r is the donor acceptor separation distance, r_0 is the sum of the van der Waals radii of the donor and acceptor, and β_{el} is a term which expresses the attenuation of κ_{el} (the electronic coupling) with increasing donor–acceptor separation. The decay of κ_n with increasing donor–acceptor separation arises primarily because of the distance dependence of λ_0 [77–80]. The Marcus–Hush two-sphere model (eqn. (6)) predicts that λ_0 increases asymptotically with increasing donor acceptor separation; however, since κ_n is a function not only of λ, but also of several other terms (see eqn. (5)), the distance dependence of κ_n depends upon many factors including λ, ΔG_{ET}, solvent polarity, and temperature. Parameters appropriate for the (bpy)Re(CO)$_3$(Pro)$_n$DMAB series were used in eqns. (5) and (6) to calculate the expected distance dependence of κ_n. This calculation suggests that κ_n should decrease asymptotically, leveling off at $r \approx 25$ Å.

From the above discussion, the distance dependence of k_{ET} can be expressed by

$$\ln k_{ET}(r) = -\beta_{el}(r - r_0) + \ln \kappa_n(r) + \ln \nu_n \tag{8}$$

Note that, due to the expected asymptotic behavior of $\kappa_n(r)$, the overall distance dependence of k_{ET} is not necessarily described by a simple exponential decay. Figure 7(a) shows the experimental rate data for the (bpy)Re(CO)$_3$(Pro)$_n$DMAB series plotted as a function of the length of the peptide spacer. The best fit line drawn through the points has a slope of 1.0 ± 0.1 Å^{-1}. Unfortunately, the data for this

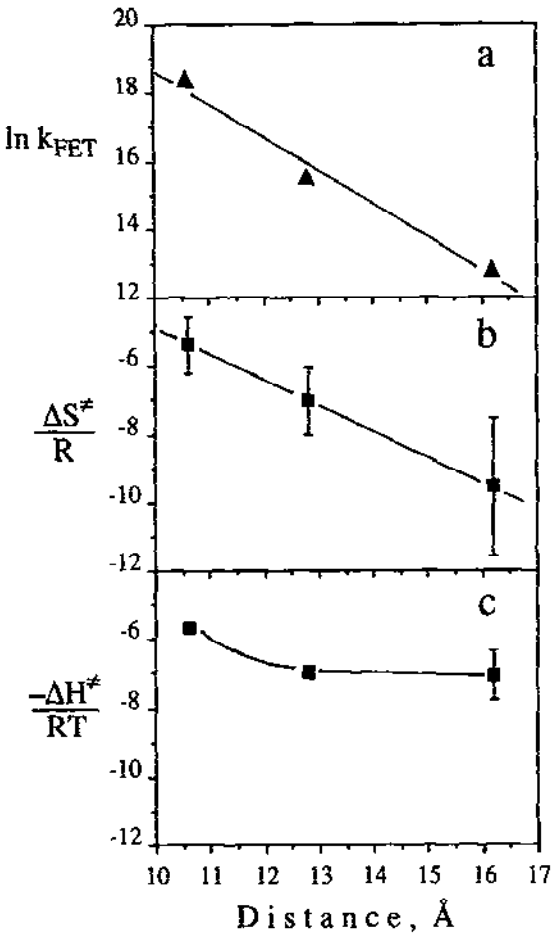

Fig. 7. Plots of (a) $\ln k_{FET}$, (b) $\Delta S^{\ddagger}_{FET}/R$, and (c) $-\Delta H^{\ddagger}_{FET}/RT$ as functions of the separation distance between the DMAB donor and the Re center for (bpy)Re(CO)$_3$PyDMAB and the (bpy)Re(CO)$_3$(Pro)$_n$DMAB complexes.

series are insufficient to determine whether the log plot is truly linear or if it displays upward curvature, as might be anticipated based on the above discussion.

Sutin has argued that, if the standard entropy change (ΔS°) for an e.t. reaction is approximately zero, then the distance dependence of κ_{el} and κ_n can be separated by examining the distance dependence of $\Delta S^{\ddagger}_{ET}$ and $\Delta H^{\ddagger}_{ET}$ [77,81] The following equations provide the relationship between the experimental activation parameters and κ_{el} and κ_n,

$$\ln \kappa_{el}(r) = \frac{\Delta S^{\ddagger}_{ET}(r)}{R} = -\beta_{el}(r - r_0) + \ln \kappa^0_{el} \tag{9a}$$

$$\ln \kappa_n(r) = -\frac{\Delta H^{\ddagger}_{ET}(r)}{RT} \tag{9b}$$

where κ_{el}^0 is the electronic transmission coefficient when the donor and acceptor are separated by the sum of their van der Waals radii, and the other parameters are defined above. Note that eqn. (9a) implies that the distance dependence of the activation entropy term allows determination of β_{el}. Figure 7(b) and (c) show plots of the experimental activation parameters according to eqns. (9). The plot of $\Delta S_{ET}^{\ddagger}/R$ is linear and the slope yields $\beta_{el} \approx 0.7$ Å^{-1}. This plot implies that electronic coupling in the proline-bridged complexes decays exponentially with increasing donor–acceptor separation, consistent with the prediction of superexchange theory. Furthermore, the observed β_{el} value is comparable with values observed for e.t. across other saturated bridges comprised of rigid C–C σ-bond frameworks, suggesting that the peptides are not significantly different from other saturated σ-bond spacers with respect to their ability to mediate electronic coupling between an electron donor and acceptor [3,9,58,65]. By contrast, the plot of $-\Delta H_{ET}^{\ddagger}/RT$ is not linear; $\Delta H_{ET}^{\ddagger}$ increases on going from zero to one proline spacer, but does not change significantly between one and two peptide spacers. These data imply that κ_{el} does not depend strongly upon distance in this system; however, since only three compounds were examined in this study, it is not possible to draw definitive conclusions concerning the distance dependence of the activation enthalpy term.

(c) *Donor-to-metal electron transfer across a rigid organic spacer*

Although peptides provide a synthetically attractive spacer system, any interpretation of the effect of spacer length on k_{ET} must take into account the complicating feature that peptides are not completely rigid and very likely undergo slow changes in conformation [42]. Thus, in order to mitigate the problem of spacer flexibility, a synthetic methodology was developed which allows attachment of the (b)Re(CO)$_3$ chromophore to a donor via rigid organic spacers [45,48]. Initial synthetic efforts led to the preparation of the series of complexes, (b)Re(CO)$_3$CH-DTF, which contain the Re(I) chromophore covalently linked to a benzo-1,3-dithiafulvene (DTF) electron donor via a *trans*-cyclohexane spacer. In this series of complexes, the center-to-center separation distance between the metal center and the DTF donor is fixed at 16 Å by the cyclohexane spacer and the dependence of k_{FET} and k_{BET} on thermodynamic driving force was examined by varying the diimine ligand at the Re(I) center.

While the synthetic methodology which was developed in the preparation of the (b)Re(CO)$_3$CH-DTF complexes is general and allows preparation of a wide variety of Re(I)–Spacer–Donor type compounds [48], there are several problems with the DTF-substituted spacer system which became apparent during these studies. First, the DTF$^{0/+}$ oxidation is irreversible on the electrochemical timescale. As a result, thermodynamic potentials are not easily accessible for the donor moiety, only peak potentials are available. Second, a more insidious problem arises due to the presence of the styryl-pyridine moiety in the spacer unit. The styryl-pyridine chromophore possesses a relatively low-lying $^3(\pi,\pi^*)$ excited state that quenches the Re → dii-

mine MLCT state for complexes with $E_{0,0} > 18\,000\ cm^{-1}$. Studies indicate that the MLCT quenching occurs via intramolecular energy transfer [48]. This problem restricts the range of diimine ligands which can be utilized to prepare a series of (b)Re(CO)$_3$CH-DTF complexes for examination of the free-energy dependence of e.t.

Table 3 contains a summary of thermodynamic and kinetic data for photo-induced forward and back e.t. in two (b)Re(CO)$_3$CH-DTF complexes. While extensive data is not available concerning the dependence of k_{ET} on ΔG_{ET} due to the problem with intramolecular energy transfer noted above, several trends are apparent in the data. First, despite the relatively large distance which separates the DTF donor and the Re center, both forward and back e.t. occur relatively rapidly. In addition, note that k_{FET} increases as ΔG_{FET} becomes more exothermic, while k_{BET} increases as ΔG_{BET} becomes less exothermic. These observations are consistent with the fact that forward e.t. is in the normal region, while back e.t. is in the inverted region. The relatively small $\Delta H^{\ddagger}_{FET}$ and large negative $\Delta S^{\ddagger}_{FET}$ values observed for both complexes suggest that forward e.t. is non-adiabatic and, further, that the rate is restricted primarily due to weak electronic coupling between the donor and the metal center.

(vi) Comparisons of forward electron transfer rate data

Table 4 contains a comparison of e.t. rate parameters for forward e.t. in the Re(I) based systems described above with the analogous parameters for e.t. in several other organic-based D–spacer–A molecules and one modified protein system [7,8,11,65]. Of most interest in such a comparison is $\nu_n \kappa_{el}$ (or H_{AB}), which reflects the propensity of the spacer to mediate electronic coupling between the donor and acceptor [58,59]. The systems chosen for comparison have comparatively rigid spacers and the dependence of k_{ET} on ΔG_{ET} has been carried out in sufficient detail to allow approximation of $\nu_n \kappa_{el}$ and λ.

Comparison of the data among the four Re(I)-based systems suggests that the electronic coupling decreases uniformly with the number of σ-bonds which separate the π systems of the donor and the metal center. Note that the electronic coupling appears to be similar for the mono-proline and cyclohexane-bridged systems which have comparable numbers of intervening σ-bonds. The differences in the structure of the donor and the spacer in the two molecules appears not to have a substantial effect on the magnitude of the electronic coupling. Comparison of the data for the Re(I)-based and the organic systems indicates that electronic coupling is similar for molecules with a similar number of intervening σ-bonds. Since, through σ-bond donor–acceptor coupling predominates in these rigid organic-based systems [82–85], the similarity in the magnitude of electronic coupling which is apparent in Table 4 implies that through-bond (as opposed to through-space) pathways predominate for the Re(I) based systems as well. Finally, it is of interest to note that electronic coupling is substantially larger in all of the D–spacer–A small molecules compared with the modified protein a$_5$Ru(His48)Mb, despite the fact that the overall donor–

TABLE 3

Electron transfer rate data for cyclohexane-bridged complexes[a]

Complex	ΔG_{FET} /eV	k_{FET}/s^{-1}	$\Delta H^{\ddagger}_{FET}$ /kcal mol^{-1}	$\Delta S^{\ddagger}_{FET}$ /eu	ΔG_{BET} /eV	k_{BET}/s^{-1}
(bpz)Re(CO)$_3$CH-DTF	−0.43	9.1(1) × 10^7	2.3(0.2)	−14(2)	−1.62	3.6(0.3) × 10^7
(4-dab)Re(CO)$_3$CH-DTF	−0.26	2.3(0.2) × 10^7	3.3(0.2)	−14(2)	−1.96	1.3(0.2) × 10^7

[a] All measurements represent averages; standard deviations are given in parentheses. All measurements carried out in MeCN solution.

TABLE 4

Comparison of electron transfer rate data

Compound[a]	Solvent	$\approx r_{cc}$/Å[b]	Number of σ-bonds[c]	$\nu_n \kappa_{el}/s^{-1}$[d]	$\approx H_{AB}/cm^{-1}$[d]	λ/eV[d]	Ref.
(b)Re(CO)$_3$PyDMAB[e]	MeCN	11	4	1.4×10^{10}	7.5	1.0	46
(b)Re(CO)$_3$CH-DTF	MeCN	16	5	6.4×10^{9}[f]	5[f]	1.0[f]	45
(bpy)Re(CO)$_3$(Pro)$_1$DMAB	MeOH	13	6	6.4×10^{9}[f]	5[f]	1.0[f]	44
(bpy)Re(CO)$_3$(Pro)$_2$DMAB	MeOH	16	9	2.6×10^{8}[f]	1[f]	1.0[f]	44
ZnTPP-(TRP)-Q	n-PrCN	10	2	3.0×10^{10}	30	0.9	8
ZnTPP-(BCO)-Q	MeCN	16	5	5×10^{9}	4	1.3	7
Bi-(Ste)-A	2-MeTHF	17.5	10	8.5×10^{9}	6	1.2	65
a$_5$Ru(His48)Mb(P*)	H_2O	13	>50	3.5×10^{5}	0.05	1.4	11

[a] Abbreviations: ZnTPP = meso-tetraphenylporphyrin Zn(II); TRP = trypticene; Q = 1,4-benzoquinone; BCO = bicylo[2.2.2]octane; Bi = biphenyl; A = various electron acceptors; Ste = steroid; a$_5$Ru(His48)Mb(P) = myoglobin derivatized at His 48 with $Ru(NH_3)_5$.

[b] Center-to-center separation distance.

[c] Number of σ-bonds separation π systems of the donor and acceptor.

[d] Estimated from dependence of k_{ET} on ΔG_{ET} unless otherwise indicated.

[e] The parameters for (b)Re(CO)$_3$PyDMAB were derived from data for the series of Re(I) complexes where b = tmb, dmb, byy, 4-dab, deb and bpz.

[f] Estimated from temperature dependence of k_{ET}.

acceptor separation distance is similar in all of the systems [11]. This large difference clearly reflects the fact that electronic coupling through the disordered protein matrix is significantly smaller than when a direct through-bond pathway exists. This finding suggests that peptide-bridged small molecules may be poor models for providing insight concerning e.t. pathways in proteins. Because electronic coupling is so much smaller in proteins compared with peptide-bridged systems, small structural effects which could enhance coupling in a disordered protein matrix might not have an effect in peptides where comparatively strong through σ-bond coupling dominates the coupling pathway.

(vii) Comparisons of back electron transfer rate data

A very interesting feature emerges when all of the available rate data for back e.t. in donor-substituted Re(I) complexes is compared. Figure 8 illustrates a plot of log k_{BET} vs. ΔG_{BET} for the three series of complexes (b)Re(CO)$_3$PyDMAB, (b)Re(CO)$_3$-CH-DTF, and (b)Re(CO)$_3$PyPTZ. Note that all of the data fall very close to the same correlation! The fact that the rate data for the (b)Re(CO)$_3$PyDMAB and (b)Re(CO)$_3$PyPTZ systems fall close to the same correlation is not surprising because the length and chemical composition of the spacer which separates the donors from the Re center is similar for the two series, and therefore electronic coupling might be expected to be similar. However, it is surprising that back e.t. is nearly as fast for the cyclohexane-bridged system, where electronic coupling might be expected to be significantly smaller. It is important to note that, for all of the three Re(I)-based

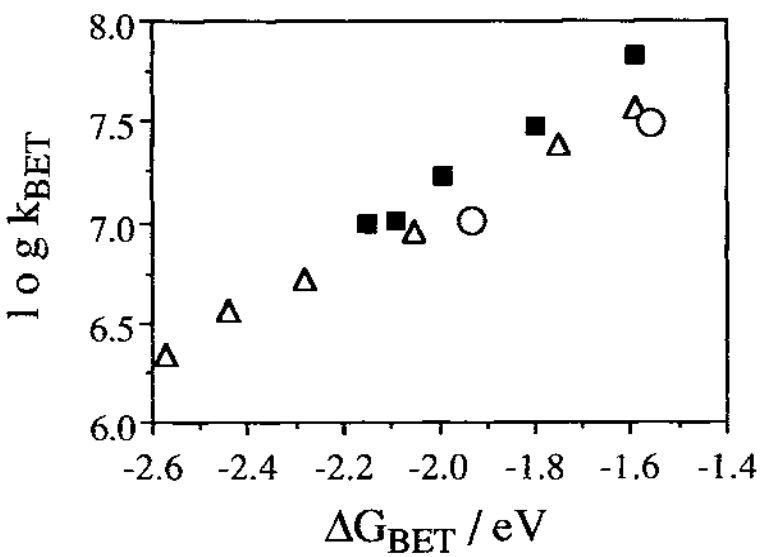

Fig. 8. Plot of log k_{BET} vs. ΔG_{BET} for donor-substituted Re(I) complexes in CH_2Cl_2 solution. △, (b)Re(CO)$_3$PyDMAB series; ○, (b)Re(CO)$_3$CH-DTF series; ■, (b)Re(CO)$_3$PyPTZ series.

systems, laser flash photolysis experiments show unequivocally that the reported rates correspond to decay of the LLCT state [24 27,45,46]. The assumption is that the observed rate is equal to k_{BET}. The correspondence of the rate data shown in Fig. 8 suggests that this assumption may be incorrect; some factor other than e.t. may be the rate-determining step for decay of the LLCT state. As noted above, one possible candidate for the rate-determining step might be ISC, the rate of which may depend upon the energy gap between the LLCT state and the ground state. In any case, further experiments are required to allow complete understanding of the unusual behavior of back e.t. in the Re(I)-based compounds.

D. INTRAMOLECULAR ENERGY TRANSFER IN Re(I) COMPLEXES

As noted above, E_{MLCT} for the (b)$Re^{I}(CO)_3$ chromophore can be tuned over a substantial range by varying the electron demand (LUMO energy) of the diimine ligand. This effect is illustrated in Fig. 2, which contains a plot of E_{MLCT} vs $E_{1/2}(Re^{+/0})$. In a recent study, we have taken advantage of the ability to tune E_{MLCT} to examine the driving force dependence of the rate of energy transfer (k_{E_nT}) from the (b)$Re(CO)_3$ chromophore to an anthracene (An) chromophore in the series of complexes (b)ReAn [47]. In this series, photoexcitation of the $d\pi(Re) \rightarrow \pi^*$ MLCT excited state is followed by rapid, intramolecular E_nT to the covalently attached An moiety:

$$(b)Re^{I}(CO)_3-An \xrightarrow{h\nu} (b^{-})Re^{II}(CO)_3-An \xrightarrow{k_{E_nT}} (b)Re^{I}(CO)_3-{}^3(An)^* \qquad (10)$$

This triplet–triplet E_nT reaction presumably occurs via the Dexter exchange mechanism [86]. The An chromophore was selected as the energy acceptor because (1) its triplet energy (E_T) is very low (1.79 eV) which results in E_nT being strongly exothermic [87], and (2) the triplet state can be easily characterized by its strong triplet–triplet absorption which appears at 420 nm [88].

That intramolecular E_nT occurs in the (b)$Re(CO)_3$An complexes is supported by several lines of evidence. First, the MLCT emission of the An-substituted complexes is strongly quenched compared with the (b)$Re(CO)_3$PyPh model complexes which do not contain the An chromophore. Second, nanosecond laser excitation of the (b)$Re(CO)_3$An complexes at a wavelength where >90% of the light is absorbed by the metal complex chromophore leads to prompt ($k > 10^8\ s^{-1}$) formation of ^{3}(An)* (see Fig. 9). Third, quenching by a competitive e.t. pathway from An to the photoexcited Re complex pathway is deemed to be unimportant for most of the complexes due to thermodynamic considerations (vide infra).

Rates for quenching of the MLCT excited state (k_q) of the (b)$Re(CO)_3$An series were determined from emission lifetimes of the (b)$Re(CO)_3$An complexes and the (b)$Re(CO)_3$PyPh model complexes by using the equation

$$k_q = \frac{1}{\tau_{em}} - \frac{1}{\tau_{em}^{model}}$$

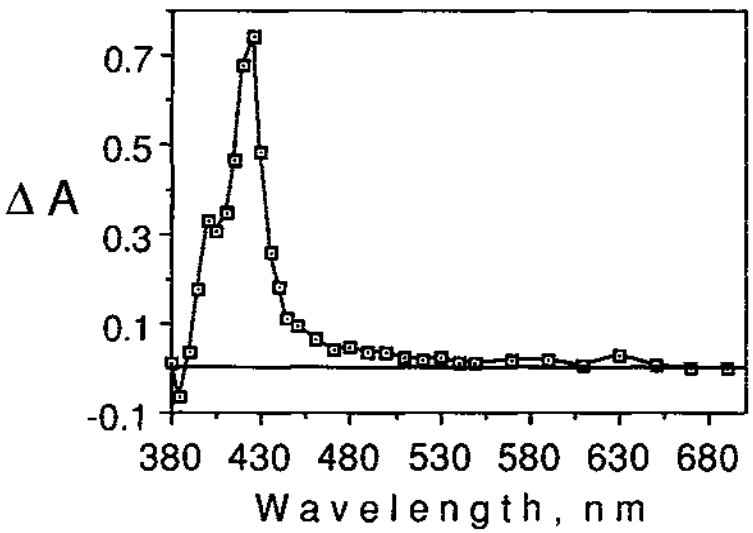

Fig. 9. Transient absorption-difference (ΔA) spectrum of (bpy)Re(CO)$_3$An ($c = 5 \times 10^{-5}$ M, MeCN solvent) obtained 200 ns following 320 nm excitation (5 mJ/pulse, 6 ns fwhm). Spectrum is identical to published ΔA spectrum of ^{3}An* [86].

The energy gap for the E_nT process was determined from the equation

$$\Delta E_{E_nT} = E_T - E_{0,0}$$

where the $E_{0,0}$ values were determined from the MLCT emission spectra of the (b)Re(CO)$_3$PyPh complexes, and E_T was assumed to be 1.79 eV [87]. Figure 10 shows a plot of k_q vs ΔE_{E_nT}; note that the rate *increases* as the energy gap *decreases*. This behavior is qualitatively consistent with predictions based on quantum-mechanical theories of non-radiative processes such as excited state decay and E_nT [60,89]. Importantly, the quantum theories predict an inverted region for E_nT which is the direct analogy of the inverted region for e.t., which has been experimentally verified [60,89]. The (b)Re(CO)$_3$An series is the first system to provide solid experimental evidence for the inverted region for an intramolecular E_nT reaction.

Despite this exciting result, there are still some unusual features concerning the correlation of k_q vs ΔE_{E_nT} displayed in Fig. 10. The solid line in the figure was calculated using a quantum mechanical expression with spectroscopic parameters that are in accord with the Re MLCT and An chromophores [47,89]. An important point is that, since the E_nT reaction is expected to have a total reorganization energy of $\approx$0.4 eV, the theory predicts that the rates should reach a maximum and begin to slow down for $\Delta E_{E_nT} > -0.4$ eV. As can be seen from Fig. 10, this is clearly not the case; k_q increases monotonically along the entire series of (b)Re(CO)$_3$An complexes.

In order to understand this apparent anomaly, electrochemical experiments

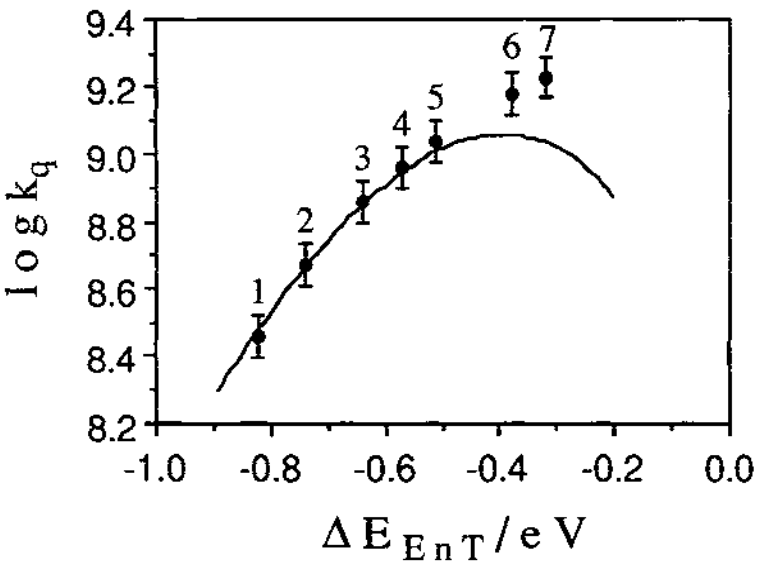

Fig. 10. Plot of log k_q vs. ΔE_{E_nT} for (b)Re(CO)$_3$An series in 2-MeTHF solution. 1, b = tmb; 2, b = dmb; 3, b = bpy; 4, b = 4-dab; 5, b = 5-dab; 6, b = deb; 7, b = bpz. Solid line calculated using quantum-mechanical expression for E_nT [47].

were carried out to allow estimation of the driving force (ΔG_{ET}) for forward e.t. from An to the photoexcited Re complex [47]. These measurements indicate that the e.t. reaction is slightly endothermic for b = tmb, dmb, bpy, and 4-dab, but becomes weakly exothermic for b = 5-dab, deb, and bpz. On this basis we postulated that e.t. may be competitive with E_nT for the latter members of the (b)Re(CO)$_3$An series, and, as a result, $k_q > k_{E_nT}$ for these complexes. Although the products of an excited-state e.t. reaction were not directly observed by laser flash photolysis, evidence that a reaction occurs which competes with E_nT to quench the MLCT state in some of the (b)Re(CO)$_3$An complexes was provided by transient absorption experiments in which the relative quantum yield for formation of ^{3}(An)*, Φ_T^{rel}, was determined for the series of complexes (Fig. 11). As can be seen from this figure, Φ_T^{rel} is nearly constant for b = tmb, dmb, and bpy, but decreases along the latter members of the series. The relative quantum yield experiments suggest that $k_{E_nT} \approx k_q$ for b = tmb, dmb, and bpy, and $k_{E_nT} < k_q$ for the other complexes.

E. CONCLUDING REMARKS

This review highlights the utility of the (b)Re^I(CO)$_3$ chromophore in studies focused on examining quantitative aspects of the mechanism of intramolecular energy and electron transfer. The utility of the Re(I) chromophore stems from several factors which include (1) clear-cut methods for synthesis and purification of a variety of

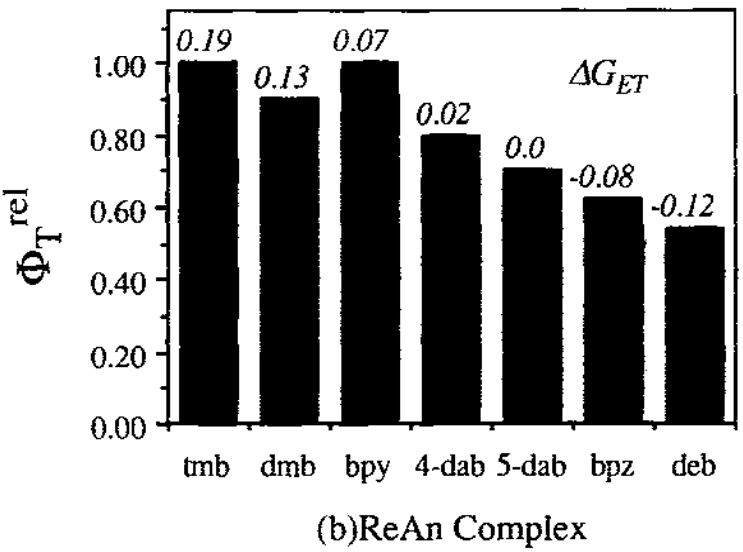

Fig. 11. Bar graph of relative quantum yield for formation of ^{3}An* for (b)Re(CO)$_3$An complexes. Numbers indicate approximate free-energy change for forward e.t. (ΔG_{ET}) for each complex.

substituted analogs, (2) a relatively long-lived, luminescent MLCT excited state, (3) tunable excited-state energy and redox potentials, and (4) photochemical stability. While this system has some shortcomings, it is clearly a useful addition to the toolbox of the inorganic photochemist who is interested in preparing supramolecular assemblies for the study of excited state energy- and charge-transfer processes.

ACKNOWLEDGEMENTS

We gratefully acknowedge the donors of the Petroleum Research Fund, administered by the American Chemical Society, for supporting our work in the area of photoinduced intramolecular electron and energy transfer.

REFERENCES

1 D. Gust and T.A. Moore (Eds.), Tetrahedron, 45 (1989) 4669–4912.
2 For a recent compilation of work on electron transfer see Adv. Chem. Ser., 228 (1991).
3 H. Oevering, M.N. Paddon-Row, M. Heppener, A.M. Oliver, E. Cotsaris, J.W. Verhoeven and N.S. Hush, J. Am. Chem. Soc., 109 (1987) 3258.
4 D. Gust and T. A. Moore, Adv. Photochem., 16 (1991) 1.
5 J.R. Bolton, J.A. Schmidt, T.-F. Ho, J. Liu, K.J. Roach, A.C. Weedon, M.D. Archer, J.H. Wilford and V.P.Y. Gadzekpo, Adv. Chem. Ser., 228 (1991) 117.
6 H. Heitele and M.E. Michel-Beyerle, J. Am. Chem. Soc., 107 (1985) 8286.
7 A.R. Joran, B.A. Leland, P.M. Felker, A.H. Zewail, J.J. Hopfield and P.B. Dervan, Nature, 327 (1987) 508.

8 M.R. Wasielewski, M.P. Niemczyk, W.A. Svec and E.B. Pewitt, J. Am. Chem. Soc., 107 (1985) 1080.
9 S. Knapp, T.G. Murali Dhar, J. Albaneze, S. Gentemann, J.A. Potenza, D. Holten and H.J. Schugar, J. Am. Chem. Soc., 113 (1991) 4010.
10 G. McLendon, Acc. Chem. Res., 21 (1988) 160.
11 B.E. Bowler, A.L. Raphael and H.B. Gray, Prog. Inorg. Chem., 38 (1990) 259.
12 M.J. Natan, W.W. Baxter, D. Kuila, D.J. Gingrich, G.S. Martin and B.M. Hoffman, Adv. Chem. Ser., 228 (1991) 201.
13 N. Mataga, Adv. Chem. Ser., 228 (1991) 91.
14 Y. Zeng and M.B. Zimmt, J. Am. Chem. Soc., 113 (1991) 5107.
15 J. Rodriguez, C. Kirmaier, M.R. Johnson, R.A. Freisner, D. Holten and J.L. Sessler, J. Am. Chem. Soc., 113 (1991) 1652.
16 H.E. Zimmerman, T.D. Goldman, T.K. Hirzel and S.P. Schmidt, J. Org. Chem., 45 (1980) 3933.
17 S.A. Latt, H.T. Cheung and E.R. Blout, J. Am. Chem. Soc., 87 (1965) 995.
18 F.P. Schwartz, M. Gouterman, Z. Muljiani and D.H. Dolphin, Bioinorg. Chem., 2 (1972) 1.
19 L. Stryer and R.P. Haughland, Proc. Natl. Acad. Sci., U.S.A., 58 (1967) 719.
20 For a recent review of metal-complex based systems see: V. Balzani and F. Scandola, Supramolecular Photochemistry, Ellis Horwood, New York, 1991.
21 B.P. Sullivan, H. Abruna, H.O. Finklea, D.J. Salmon, J.K. Nagle, T.J. Meyer and H. Sprintschnik, Chem. Phys. Lett., 58 (1978) 389.
22 T.D. Westmoreland, H. LeBozec, R.W. Murray and T.J. Meyer, J. Am. Chem. Soc., 105 (1983) 5952.
23 P. Chen, E. Danielson and T.J. Meyer, J. Phys. Chem., 92 (1988), 3708.
24 T.D. Westmoreland, K.S. Schanze, P.E. Neveaux, Jr., E. Danielson, B.P. Sullivan, P. Chen and T.J. Meyer, Inorg. Chem., 24 (1985) 2596.
25 P. Chen, T.D. Westmoreland, E. Danielson, K.S. Schanze, D. Anthon, P.E. Neveaux, Jr. and T.J. Meyer, Inorg, Chem., 26 (1987) 1116.
26 P. Chen, R. Duesing, G. Tapolsky and T.J. Meyer, J. Am. Chem. Soc., 111 (1989) 8305.
27 P. Chen, R. Duesing, D.K. Graff and T.J. Meyer, J. Phys. Chem., 95 (1991) 5850.
28 R. Duesing, G. Tapolsky and T.J. Meyer, J. Am. Chem. Soc., 112 (1990) 5378.
29 S.L. Mecklenburg, B.M. Peek, B.W. Erickson and T.J. Meyer, J. Am. Chem. Soc., 113 (1991) 8540.
30 T.J. Meyer, Acc. Chem. Res., 22 (1989) 163.
31 C.M. Elliott, R.A. Freitag and D.D. Blaney, J. Am. Chem. Soc., 197 (1985) 4647.
32 L.F. Cooley, C.E.L. Headford, C.M. Elliott and D.F. Kelley, J. Am. Chem. Soc., 110 (1988) 6673.
33 L.F. Cooley, S.L. Larson, C.M. Elliott and D.F. Kelley, J. Phys. Chem., 95 (1991) 10694.
34 C.K. Ryu, R. Wang, R.H. Schmehl, S. Ferrere, M. Ludwikow, J.W. Merkert, C.E.L. Headford and C.M. Elliott, J. Am. Chem. Soc., 114 (1992) 430.
35 R.H. Schmehl, R.A. Auerbach and W.F. Wacholtz, J. Phys. Chem., 92 (1988) 6202.
36 C.K. Ryu and R.H. Schmehl, J. Phys. Chem., 93 (1989) 7961.
37 J.R. Shaw, R.T. Webb and R.H. Schmehl, J. Am. Chem. Soc., 112 (1990) 1117.
38 J.R. Shaw and R.H. Schmehl, J. Am. Chem. Soc., 113 (1991) 389.
39 R.H. Schmehl and C.K. Ryu, J. Am. Chem. Soc., in press.
40 J.S. Kreuger, J.E. Mayer and T.E. Mallouk, J. Am. Chem. Soc., 110 (1988) 8232.
41 L.S. Fox, M. Kozik, J.R. Winkler and H.B. Gray, Science, 247 (1990) 1069.
42 K.S. Schanze and K. Sauer, J. Am. Chem. Soc., 110 (1988) 1180.

43 L.A. Cabana and K.S. Schanze, Adv. Chem. Ser., 226 (1990) 101.
44 K.S. Schanze and L.A. Cabana, J. Phys. Chem., 94 (1990) 2740.
45 T.A. Perkins, B.T. Hauser, J.R. Eyler and K.S. Schanze, J. Phys. Chem., 94 (1990) 8745.
46 D.B. MacQueen and K.S. Schanze, J. Am. Chem. Soc., 113 (1991) 7470.
47 D.B. MacQueen, K.S. Schanze and J.R. Eyler, J. Am. Chem. Soc., 114 (1992) 1897.
48 T.A. Perkins, Ph.D. Dissertation, University of Florida, 1991.
49 L.A. Cabana, M.S. Thesis, University of Florida, 1992.
50 M. Furure, M. Naiki, Y. Kanematsu, T. Kushida and M. Kamachi, Coord. Chem. Rev., 111 (1991) 221.
51 J.V. Caspar, B.P. Sullivan and T.J. Meyer, Organometallics, 2 (1983) 551.
52 M. Wrighton and D.L. Morse, J. Am. Chem. Soc., 96 (1974) 998.
53 P.J. Giordano and M.S. Wrighton, J. Am. Chem. Soc., 101 (1979) 2888.
54 M.S. Wrighton and G.L. Geoffroy, Organometallic Photochemistry, Academic Press, New York, 1979, Chap. 2.
55 L.A. Worl, R. Duesing, P. Chen, L. Della Ciana and T.J. Meyer, J. Chem. Soc., Dalton Trans., (1991) 849.
56 T.J. Meyer, Prog. Inorg. Chem., 30 (1983) 389.
57 J.R. Bolton and M.D. Archer, Adv. Chem. Ser., 228 (1991) 7.
58 R.A. Marcus and N. Sutin, Biochim. Biphys. Acta, 811 (1985) 265.
59 N. Sutin, Prog. Inorg. Chem., 30 (1983) 441.
60 J. Ulstrup and J. Jortner, J. Chem. Phys., 63 (1975) 4358.
61 R.A. Marcus, J. Chem. Phys., 43 (1965) 679.
62 B.S. Brunschwig, S. Ehrenson, and N. Sutin, J. Phys. Chem., 90 (1986) 3657.
63 N.S. Hush, Trans. Faraday Soc., 57 (1961) 557.
64 J.R. Miller, J.V. Beitz and R.K. Huddleston, J. Am. Chem. Soc., 106 (1984) 5057.
65 G.L. Closs, L.T. Calcaterra, N.J. Green, K.W. Penfield and J.R. Miller, J. Phys. Chem., 90 (1986) 3673.
66 I.R. Gould, D. Ege, J.E. Moser and S. Farid, J. Am. Chem. Soc., 112 (1990) 4290.
67 E.M. Kober and T.J. Meyer, Inorg. Chem., 23 (1984) 3877.
68 C.M. Deber, F.A. Bovey, J.P. Carver and E.R. Blout, J. Am. Chem. Soc., 92 (1970) 6191.
69 E. Gross and J. Meienhofer (Eds.), The Peptides: Analysis, Synthesis, Biology, Vol. 1, Academic Press, New York, 1979.
70 S.S. Isied, A. Vassilian, R.H. Magnuson and H.A. Schwartz, J. Am. Chem. Soc., 107 (1985) 7432.
71 A. Vassilian, J.F. Wishart, B. van Hemelryck, H.A. Schwarz and S.S. Isied, J. Am. Chem. Soc., 112 (1990) 7278.
72 M. Faraggi, M.R. DeFelippis and M.H. Klapper, J. Am. Chem. Soc., 112 (1990) 5640.
73 M. S. Meier, M.A. Fox and J.R. Miller, J. Org. Chem., 56 (1991) 5380.
74 M. Sisido, R. Tamaka, Y. Inai and Y. Imanishi, J. Am. Chem. Soc., 111 (1989) 6790.
75 H.M. McConnell, J. Chem. Phys., 35 (1961) 508.
76 N. Sutin, Adv. Chem. Ser., 228 (1991) 25.
77 S.S. Isied, A. Vassilian, J.F. Wishart, C. Creutz, H.A. Schwarz and N. Sutin, J. Am. Chem. Soc., 110 (1988) 635.
78 T.J. Meyer, Prog. Inorg. Chem., 30 (1983) 389.
79 D.A. Geselowitz, Inorg. Chem., 26 (1987) 3639.
80 G.-H. Lee, L. Della Ciana and A. Haim, J. Am. Chem. Soc., 111 (1989) 2535.
81 J.T. Hupp and M. Weaver, Inorg. Chem., 23 (1984) 256.
82 P. Siddarth and R.A. Marcus, J. Phys. Chem., 94 (1990) 2985.
83 K. Ohta, G.L. Closs, K. Morokuma and N. Green, J. Am. Chem. Soc., 108 (1986) 1319.

84 D.N. Beratan, J. Am. Chem. Soc., 108 (1986) 4321.
85 S. Larsson and A. Volosov, J. Chem. Phys., 85 (1986) 2548.
86 D.L. Dexter, J. Chem. Phys., 21 (1953) 866.
87 M.R. Padhye, S.P. McGlynn and M. Kasha, J. Chem. Phys., 24 (1956) 588.
88 D.S. Kliger and A.C. Albrecht, J. Chem. Phys., 53 (1970) 4059.
89 G. Orlandi, S. Monte, F. Barigelletti and V. Balzani, Chem. Phys., 52 (1980) 313.